A Self-Calibrated Localization System using Chirp Spread Spectrum in a Wireless Sensor Network

Seong-Joong Kim[1] and Dong-Joo Park[1]
[1] School of Computer Science and Engineering, Soongsil University
#369 Sangdo-dong, Dongjak-gu, Seoul 156-743, South Korea
[e-mail: haru8988@gmail.com, djpark@ssu.ac.kr]
*Corresponding author: Seong-Joong Kim

Received June 4, 2012; revised September 28, 2012; accepted January 20, 2013; published February 26, 2013

Abstract

To achieve accurate localization information, complex algorithms that have high computational complexity are usually implemented. In addition, many of these algorithms have been developed to overcome several limitations, e.g., obstruction interference in multi-path and non-line-of-sight (NLOS) environments. However, localization systems those have complex design experience latency when operating multiple mobile nodes occupying various channels and try to compensate for inaccurate distance values. To operate multiple mobile nodes concurrently, we propose a localization system with both low complexity and high accuracy and that is based on a chirp spread spectrum (CSS) radio. The proposed localization system is composed of accurate ranging values that are analyzed by simple linear regression that utilizes a Big-O(n^2) of only a few data points and an algorithm with a self-calibration feature. The performance of the proposed localization system is verified by means of actual experiments. The results show a mean error of about 1 m and multiple mobile node operation in a 100×35 m^2 environment under NLOS condition.

Keywords: Localization system, wireless sensor network, location estimation system, chirp spread spectrum, IEEE 802.15.4a

http://dx.doi.org/10.3837/tiis.2013.02.005

1. Introduction

With the development of ubiquitous industries and technologies, many studies have been conducted on the sensitivity of sensor devices and techniques for communication networks. Among them, research on indoor localization systems has provided useful advances in many areas, such as monitoring, servicing, and management infrastructures for industries. In hospitals and industrial plants, in particular, real-time location information from important devices can provide useful data that can play important roles in various areas. Automated AGV, in which mobile robots follow markers or wires, is an example of the application of a localization system [1]. At present, indoor localization systems and location tracking application systems are among the most important and fundamental research fields associated with wireless sensor networks.

Many studies have investigated the recognition of the localization information from mobile nodes using the angle of arrival (AoA), time of arrival (ToA), time of flight (ToF), and received signal strength indication (RSSI). The angle of arrival (AoA) measurement is a method used to determine the direction of propagation of a radio-frequency wave incident on an antenna array [2]. The time of arrival (ToA), also referred to as time of flight (ToF), is the travel time of a radio signal from a single transmitter to a remote single receiver [3]. The received signal strength indicator (RSSI) is a measure of the power present in a received radio signal [4]. These techniques are easily affected by the environment. The original signal from a transmitter reaches the receiver after being echoed and reflected from buildings and other environmental obstructions due to multipath propagation [5]. The reflections reach the receiver in or out of phase, and some frequencies are amplified or attenuated depending on the conditions, leading to a disconnection of the communication link in narrow band transmission systems.

To resolve the above problems, including the disturbance to signals that are strongly affected by obstruction interference, many algorithms have been introduced to calibrate the deficiency of conventional communication technique's. Some properties of the signals received in both the time and frequency domains are utilized in super-resolution algorithms such as the MLE algorithm and the MUSIC algorithm [6][7]. However, despite their impressive precision, super-resolution estimates involve high computational complexity and the requirement of a priori knowledge. It is therefore difficult to use these algorithm to support the operation of multiple mobile nodes due to their high computational complexity, which is caused by the calibration method used with this real-time localization system.

In recent years, many attempts have been made to improve the precision of ranging hardware techniques. Ranging methods such as ToF usually rely on the detection of the leading edge of the cross-correlation function to estimate the precise moment of signal reception. The wider the signal bandwidth, the narrower the correlation peaks. This increases the time resolution of the method, which coincides with an increase in the precision of the location [8]. This is why Ultra-Wide-Band (UWB) technology is commonly chosen for ranging systems [9]. However, there are two obstacles to consider when deploying UWB technology. First, UWB is still not close to being licensed worldwide despite the fact that the first license to use UWB communication for indoor operations in the United States was granted by the FCC in 2002. Secondly, UWB is still a very new technology that has not yet achieved wide acceptance outside of the research community. The typical performance of a

500 MHz UWB radio provides sufficiently accurate distance measurement with much less bandwidth than conventional methods. The Chirp spread spectrum (CSS) is different from UWB in that the amplified and attenuated signals are in balance because all energy shares, which are spread over a bandwidth of 80MHz, are collected in an integrated broadband technique [10]. As a result of these features, accurate range values can be obtained.

In this paper, we propose a location estimation system that has low computational complexity and high accuracy estimation capability, and localizes multiple mobile nodes using the CSS modulation technique. We flatten the measured range error to within 2 m using a simple linear regression model and apply the proposed localization algorithm, which has a self-calibration feature. The complexity of the simple linear regression analysis is Big-$O(n^2)$ for only 30 data points, and the algorithm has simple and intuitive characteristics.

In this paper, using the measurements acquired from indoor environmental experiments, we first find the characteristics of the CSS radio. Next, we apply our proposed self-calibration algorithm to the optimum condition. Our work is novel in that we consider a new type of localization system and present experimental results that show a significant improvement in the resolution accuracy compared to conventional localization systems. In addition, our algorithm makes it possible to facilitate more operations between multiple mobile nodes with low levels of complexity.

The remainder of this paper is organized as follows: in Sections 2 and 3, we describe related work and the error-distribution model for measuring the distance value. Our proposed localization system and the low-complexity, high-accuracy algorithm are described in Section 4. Performance evaluation and experimental results are outlined in Section 5. Finally, we conclude this paper in Section 6.

2. Related Work

Indoor localization systems have been actively studied over the years. The maximum likelihood estimation (MLE) method is one of the typical methods studied, and its localization accuracy is fairly high [11]. This method's principle of operation is as follows: The target node estimates its location using the MLE algorithm based on probability grids. The probability grids are created by dividing the network area (χ) into small square grids (χ_i) and calculating the probability distribution function (PDF) for each grid. The target node then chooses the grid that will most likely maximize the PDF as its estimated location. The estimated location is expressed as follows:

$$\hat{x} = \arg\max_{x_i \in X} \prod_{j=1}^{m} p(rangingvalue(i, j) \mid x_i) \tag{1}$$

Here, $p(ranging\ value(i,j) \mid x_i)$ denotes the probability distribution of each grid position (x_i) for anchor node j. **Fig. 1** shows how the target location is estimated using the position grid method. According to equation (1), the target node can estimate its location. The characteristics of the method are described in detail in [11]. However, this method has a weak point in that the computational complexity for MLE detection increases exponentially with the number of small square grids due to the multiplication operation.

Furthermore, the above methods require specific knowledge about the NLOS error distribution, and a complex training process, making them impractical for widespread

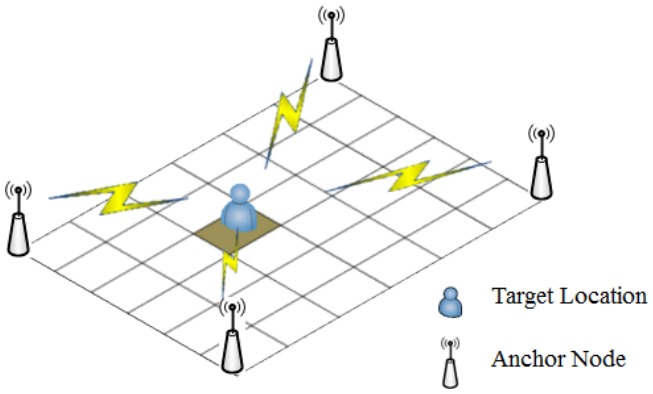

Fig. 1. Location estimation using the position grid method

adoption in indoor localization. Therefore, there is a latency problem when operating multiple mobile nodes occupying various channels. To construct a highly accurate localization system with a low level of-complexity, it is essential that precise range values are obtained. Consequently, we propose a location estimation system that is based on CSS modulation and has low complexity and high accuracy in both line-of-sight (LOS) and non-line-of-sight (NLOS) environments, and realizes multiple-mobile- node operations using simple linear regression analysis.

3. Error-Distribution Model for Elaborative CSS Ranging

The major challenges we seek to overcome are how to design a well-defined error-distribution model for CSS ranging in indoor environments and whether a specific error-distribution model can sufficiently filter or smooth estimation distances.

We experimented on CSS ranging between two nodes and analyzed how measurement errors and distributions changed while varying the distances. We also conducted an experimental analysis to characterize the measurement error, as accurate predictions of a signal path are not possible during multi-path propagation. By means of these experiments, we determined the limitations of CSS ranging and devised a solution to overcome these defects in an effort to compose a robust and practical localization system.

We conducted experiments with CSS ranging hardware to evaluate the characteristics of the range measurements under line-of-sight (LOS) and non-line-of-sight (NLOS) conditions in indoor building environments. The first site, a LOS environment, was an obstacle-free indoor hall that had close to ideal conditions. The second site, a NLOS environment, we considered appropriate for conducting experiments to assess CSS ranging values because all of its walls and floors were made from concrete. This location also had many obstacles, making it useful site for testing the effects of multi path propagation.

We built a device equipped with an IEEE 802.15.4a CSS compatible transceiver, a micro controller, and other peripheral devices. **Fig. 2 (a)** and **(b)** depicted the probabilistic density function of the measurement distance error in LOS and NLOS environments. **Fig. 2 (a)** shows the relatively high quality of the measured range value (the mean of error distribution is lower than 1m) and shows that the LOS range measurements have a Gaussian distribution. However, **Fig. 2 (b)** shows that the NLOS measurements are noisy; therefore, no rule can be gleaned from the data.

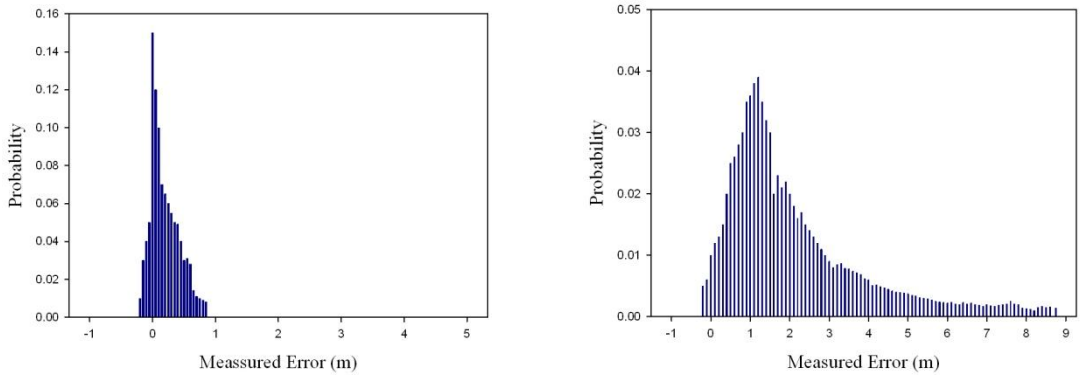

(a) (b)

Fig. 2. CSS ranging measurement errors: (a) a LOS environment, (b) an NLOS environment

We noticed abnormal ranging regions with biased errors larger than 2 m and found unstable positions that had large deviations from the results estimated in the experiment. These out-of-range positions reflect the influence of the surrounding environments on the multi-path signal propagation results. The ranging results were unreliable and likely the primary source of positioning errors.

In this paper, to solve this problem, we propose a method that reduces range error deviation using linear regression analysis; specifically, simple regression analysis. In statistics, linear regression is a means of modeling the relationship between a scalar variable *y* and one or more explanatory variables, denoted as *x*. This method is suitable for fitting the measured distance, which includes random error distribution, because a simple linear regression analysis can be used to fit a predictive model to an observed data set of *y* and *x* values. The line that fits the measured distance under the LOS and NLOS conditions can be expressed as follows:

$$y = \hat{\alpha} + \hat{\beta}x \tag{2}$$

Here, *x* is the measured range value, which includes error of some degree, and *y* is the value that is fitted by linear regression analysis. $\hat{\beta}$ is the slope, and $\hat{\alpha}$ is the intercept of this line. It can be shown that the values of $\hat{\alpha}$ and $\hat{\beta}$ are given by

$$\hat{\alpha} = \overline{Y} - \hat{\beta}\overline{x} \quad \text{and} \quad \hat{\beta} = \frac{\sum_{i=1}^{n}(x_i - \overline{x})(Y_i - \overline{Y})}{\sum_{i=1}^{n}(x_i - \overline{x})^2} \tag{3}$$

where

$$\overline{x} = \frac{\sum_{i=1}^{n} x_i}{n}, \quad \overline{Y} = \frac{\sum_{i=1}^{n} Y_i}{n}, \text{ and } n = \{ \textit{the number of data} \} \tag{4}$$

The simple linear regression model was applied to the measured range value for 30 data

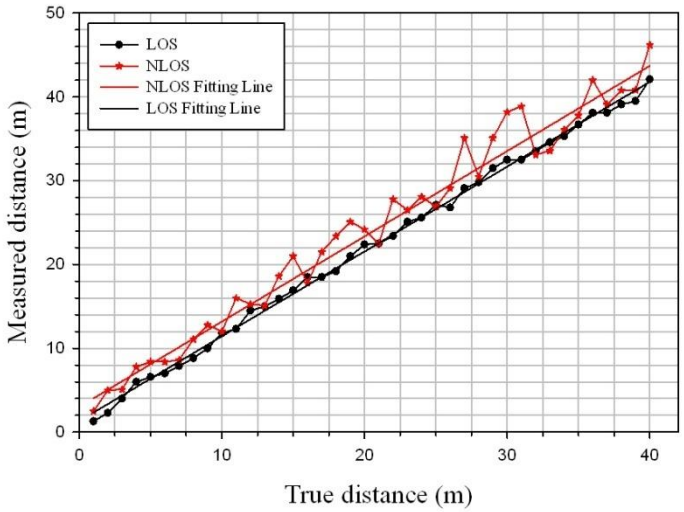

Fig. 3. Fitted lines for the LOS and NLOS conditions using a real-time linear regression model

points in real time. The regressed range value in the NLOS fitting line in **Fig. 3** measures a mean error of about 2 m from the true distance under indoor building environment. This served as a fine source for composing an outstanding localization system. In addition, the regression model required the complex computation only in the form of Big-$O(n^2)$ for only 30 data points, refer to (3) and (4) .

Using this technique, we improved the value of the error deviation that converges to a mean error value of approximately 2 m even in the NLOS environment. In the next Section, we propose a localization algorithm that shows that the positional error of the mobile node is approximately 1 m when the measuring distance values with error deviation of approximately 2 m are used.

4. Self-Calibrated Localization Scheme

4.1 System Operation and Architecture

The system architecture of the scheme is depicted in **Fig. 4 (a)**. The proposed indoor localization system using a CSS radio consists of three types of nodes: anchor nodes (*ANs*), mobile nodes (*MNs*), and the base station node (*BSN*). *MNs* are attached to people or things and are thus in continuous motion. These nodes can communicate with the *ANs*, which are located in fixed positions, and can obtain the leading edge detection ranging values using the CSS radio technique. The *BSN* is used to configure and control the operation of the proposed network system. It can monitor the location of the *MNs*, which are in continuous motion, as well as the status of each node that is not in operation.

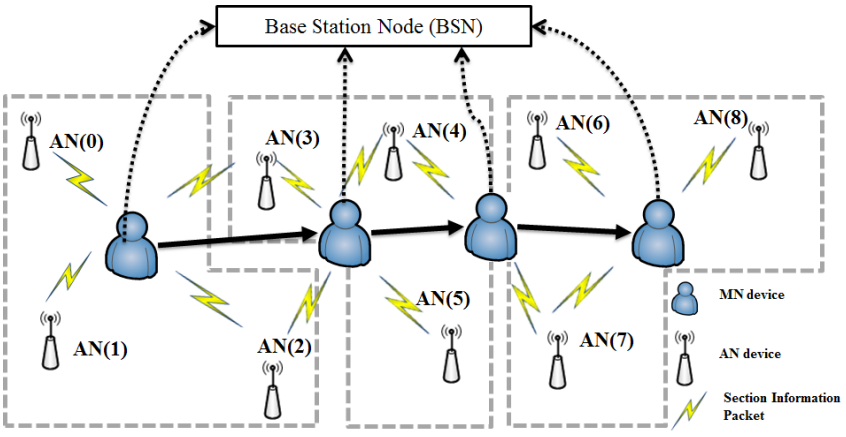

Packet Type	Contents	Description
Section A Information Packet	AN(0), AN(1), AN(2)	Each AN's Address
Section B Information Packet	AN(3), AN(4), AN(5)	Each AN's Address
Section C Information Packet	AN(6), AN(7), AN(8)	Each AN's Address

(a)

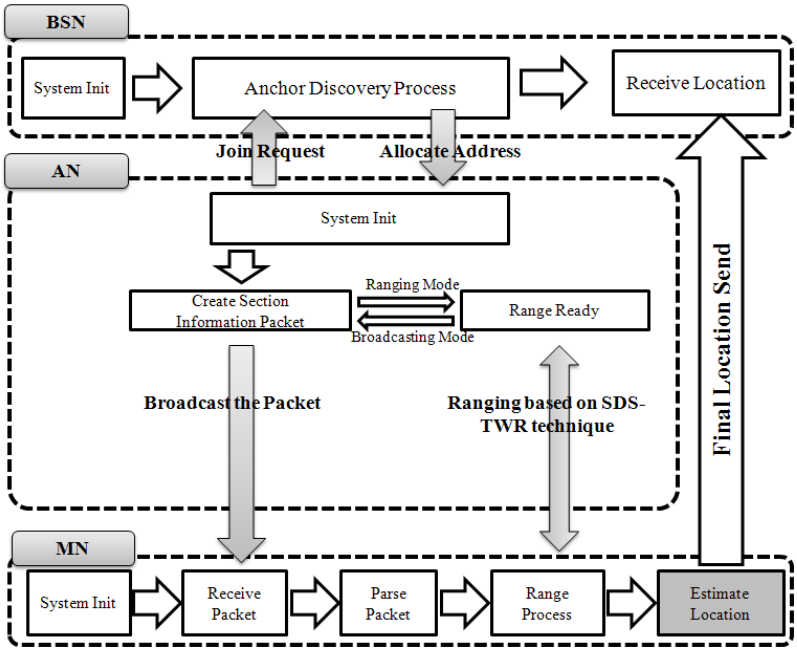

(b)

Fig. 4. (a) Conceptual diagram and (b) system operation of the localization system using the proposed method

First, the *BSN* sets the logical address of each *AN*s and then starts the network. Each *AN* initializes with a distinct address allocated by the *BSN* and joins the network using a *join request* and an *address allocation* packet. When a new *AN* wishes to join the network, it requests a *join request* packet from the BSN, and the *BSN* redistributes a new logical address to each *AN* in the network. After this process, the *BSN* goes into standby mode to receive the location of the *MN*s in real-time in order to monitor the network. If device that are configured

as *AN*s by switching between two modes: the *broadcasting mode* and the *ranging mode*. In *broadcasting mode*, a *section information packet* which includes its associated section information, is broadcast to the continuously moving *MN*s, as depicted in **Fig. 4 (b)**. The section information data includes information on three arbitrary neighboring nodes. Each *AN* contains section information that includes information on these three *AN*s surrounding it. The ranging mode is used by an *AN* to communicate with an *MN* in order to obtain ranging values. The *AN* enters the ranging mode for a while then switches to the *broadcasting mode* to broadcast its *section information packet*. The *MN* that receives the *section information packet*, first parses the packet to obtain the location information of each *AN*. It then makes a request to enter the ranging process with its surrounding *AN* devices, after which the *MN* device can determine the distance between each of the *AN* and *MN* devices using the SDS-TWR method [12].

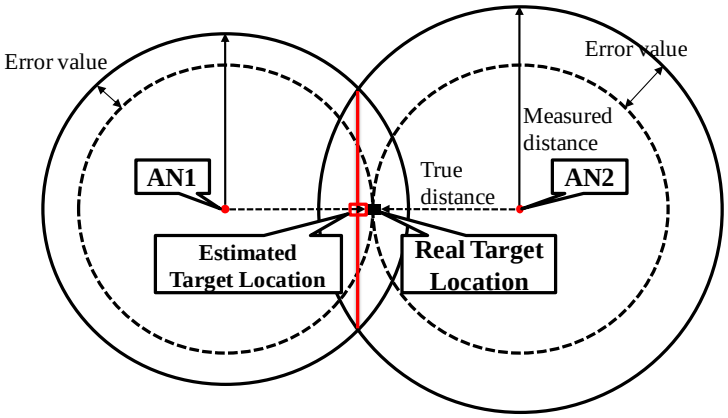

Fig. 5. Concept of the proposed localization scheme

Let us now look at our proposed algorithm, which is based on the calibrated CSS range value and uses a simple linear regression analysis. **Fig. 5** shows two circle, each with an *AN* at its center using the measured distance, which is the calculated value between each *AN* and *MN* using CSS ranging hardware. In the figure, a line is drawn between the two points at which the circles intersect. We consider the estimated *MN*'s location to be on this straight line. This method encompasses a self-calibration feature that takes into consideration the error in the measured distance value for the localization information of the *MN*s.

4.2 Proposed Localization Algorithm based on a Polar Coordinate System

After obtaining the location information for three arbitrary neighboring *AN*s, we try to estimate the *MN*'s location. The proposed localization algorithm is described within a polar coordinate system because it recognizes the positions of mobile nodes using only the angle and distance information from a specific point (e.g., point of origin). The proposed algorithm has two phases: conversion of the Cartesian coordinates to a polar coordinate system and calculation of the estimated location of the *MN* in the polar coordinate system.

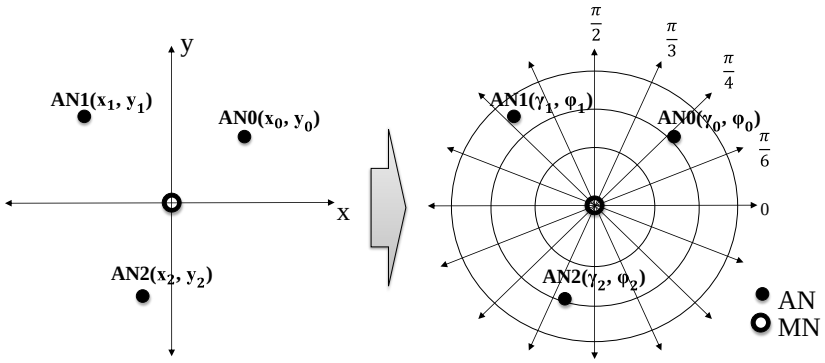

Fig. 6. Conversion between polar and Cartesian coordinates

In the first phase, we convert the conventional Cartesian coordinate system to a polar coordinate system, as depicted in **Fig. 6.** Before the conversion, we initially determine the point origin point of origin in this coordinate system, after which we calculate the location from the origin. In the Cartesian coordinate system, each point has *x* and *y* components and an angle φ from the origin. This allows the distance $\{\gamma_0=x^2+y^2\}$ to be determined from the origin in the Cartesian system, via the Pythagorean Theorem. These components, specifically the range value (γ_0) and angle (φ) from the origin, serve as elements in the polar coordinate system.

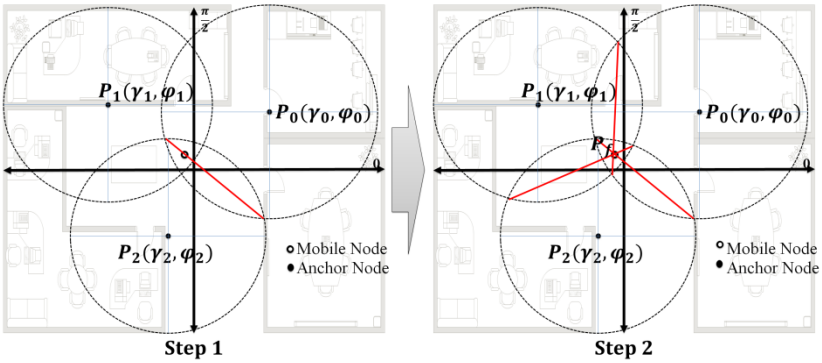

Fig. 7. Final MN device location estimation procedure

After the conversion, we formulate a circle equation with a center using the measured distance between each *AN* and *MN* device as the radius α, as follows:

$$P(\gamma_0,\varphi_0): r^2 - 2rr_0\cos(\theta-\varphi_0)+r_0^{\,2}=\alpha^2 \tag{5}$$

We can apply this method to each fixed *AN* using its location information and measured ranging information. We can also obtain the circular equation from three points: $P_0(\gamma_0, \varphi_0)$, $P_1(\gamma_1, \varphi_1)$, and $P_2(\gamma_2, \varphi_2)$, as depicted in **Fig. 7**.

Next, we calculate the final location of the *MN* using the proposed localization algorithm. To find the final location of the *MN*, we formulate the pairs $\{P_0(\gamma_0,\varphi_0), P_1(\gamma_1, \varphi_1)$, and $P_2(\gamma_2, \varphi_2)\}$ using the three circular equations $\{P_0(\gamma_0,\varphi_0), P_1(\gamma_1, \varphi_1)$, and $P_2(\gamma_2, \varphi_2)\}$. First, we will describe the process of handling the $\{P_2P_0\}$ pairs and then deal with the others.

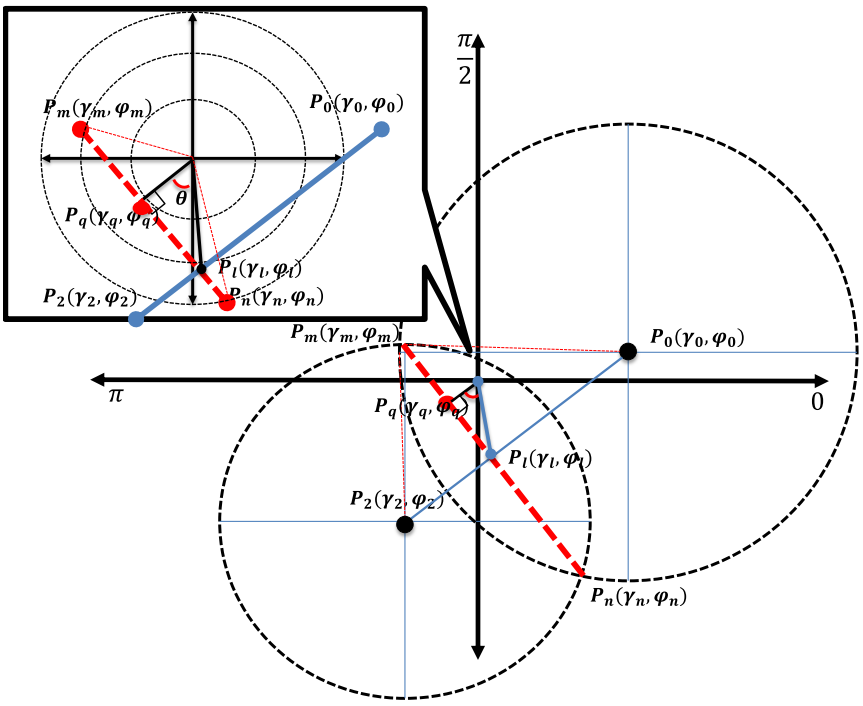

Fig. 8. More specific procedure for step 2

We can find the slope value φ as follows: We first determine P_m and P_n, the points where the two circles intersect (depicted in **Fig. 8**) using the simultaneous equations $P_0(\gamma_0,\varphi_0)$ and $P_2(\gamma_2,\varphi_2)$. The equation of the line passing through points P_m and P_n is found by using the slope of the two points. Thus, determination of the line equation in the polar coordinate system proceeds as follows:

$$r(\theta) = \gamma \cdot \sec(\theta - \varphi) \tag{6}$$

Here, φ is the angle of elevation of the line, i.e., $\{\varphi = arctan(\Phi)\}$, where Φ is the slope of the line in the Cartesian-system. The non-radial line that crosses the radial line $\{\theta = \varphi\}$ perpendicularly at the point (γ, φ) is expressed by equation (6). If we use this method, we must find the γ and φ values. Here, φ is the slope of the straight line to be determined, $(P_m \sim P_n)$ and γ is the nearest distance from the origin to the straight line we want $(P_q \sim 0)$, as depicted in **Fig. 8.**

$$\varphi = \frac{\gamma_2 \sin\varphi_2 - \gamma_0 \sin\varphi_0}{\gamma_2 \cos\varphi_2 - \gamma_0 \cos\varphi_0} \tag{7}$$

The value of φ is assigned as PI/2 when φ_0 and φ_2 are respectively PI/2 and 3PI/2, or reverse. The method used to determine distance value γ is as follows:
Let the gradient values of straight line $(P_0 \sim P_2)$ be δ and those of lines $(P_2 \sim P_0)$ and $(P_l \sim P_2)$ *be* α and β, respectively.

$$\alpha = \left[\left(\gamma_2 \cos\varphi_2 - \gamma_0 \cos\varphi_0\right)^2 + \left(\gamma_2 \sin\varphi_2 - \gamma_0 \sin\varphi_0\right)^2 \right]^{0.5} \tag{8}$$

$$\beta = \frac{\gamma_0^{\,2} - \gamma_2^{\,2} + \alpha^2}{2 \cdot \alpha}, \qquad \delta = \varphi^{-1} \tag{9}$$

The values of γ_0, γ_2, φ_0 and φ_2 are depicted in **Fig. 8**, and φ is defined in equation (7). Using the above method, P_t's x and y components are $\{\gamma_2 \cos(\varphi_2) + \beta \cos(\varphi)\}$ and $\{\gamma_2 \sin(\varphi_2) + \beta \sin(\varphi)\}$, respectively. Consequently, we can obtain the calculated distance P_0 from the origin, (P_0~0), as follows:

$$\gamma = \left[\left(\alpha \cdot \cos\varphi_0 + \beta \cdot \cos\delta \right)^2 + \left(\alpha \cdot \sin\varphi_0 + \beta \cdot \sin\delta \right)^2 \right]^{0.5} \tag{10}$$

The method above can be applied to the three circular equations $P_0(\gamma_0,\varphi_0)$, $P_1(\gamma_1,\varphi_1)$, and $P_2(\gamma_2,\varphi_2)$.

Finally, in step 1 of **Fig. 7**, we can find the intersection point of the three straight lines passing through the intersection point of the two circular equations at $P_0(\gamma_0,\varphi_0)$, $P_1(\gamma_1,\varphi_1)$, and $P_2(\gamma_2,\varphi_2)$. The point P_f, described in step 2 of **Fig. 7**, denotes the final estimated location of the *MN* using the proposed localization algorithm.

4.3 Complexity of the proposed Localization System: Comparative Study

In this Sub-Section, we analyze the computational complexity of our proposed localization system and compare it with that of the conventional method (the MLE technique that is based on the position grid method). The conventional localization system uses a statistical approach, such as the location constraints technique, for robust localization. A location constraint means a relationship between the distances of more than two reference nodes from an unknown node that determines its proximity to either of the reference nodes. In this method, the unknown node determines its location constraints using ranging values or received signal strength indicators and estimates its position by searching through grid areas in the localization space to determine the accurate grid area with the highest number of matched location constraints. Yedavalli *et al.* [13] proposed a localization system based on the grid method with cost $O(n^2S^2/r^2)$ time operation, where S is the side of the square localization space and r is the resolution of the grid areas. They subsequently proposed an enhanced localization system with cost $O(n^6)$ [14].

The computational complexity of our proposed localization system stems from calculation of the position of the *MN* devices and measurement of the ranging value between *MN* and *AN*. As shown in Section 3, the regressed range value in NLOS gives a mean error of approximately 2 m with cost $O(n^2)$. As shown in Section 4, the final position of the *MN* requires only small of arithmetic operation with cost $O(1)$. Thus, the total cost of our proposed localization system to find *MN* devices is $O(n^2)$. In the next Section, we give empirical evidence to support the performance of the operation with multiple *MN*s.

5. Experimental Results and Discussion

5.1 Simulation

To validate the feasibility of our proposed localization algorithm, which has a self-calibration feature, we evaluated the performance of the algorithm using simulations. We then verified the

proposed localization system, which consists of measuring the accurate range value and applied the algorithm in a realistic experiment.

In this paper, we created a simulation program only for applying and evaluating the proposed localization algorithm before experimental test is conducted, as depicted in **Fig. 9.** To evaluate the performance of the proposed algorithm, we conducted the simulation that the distance value has an error range of 1 m to 3 m as an input parameter and measured positional accuracy as a function of a distance error range with simulations. As discussed in Section 3, we can acquire quite accurate switch error range value within 2 m using simple linear regression analysis. Therefore, to confirm the efficacy of the algorithm, we considered a range error from 1 m to 3 m in the simulation. The simulation depicted in **Fig. 9** shows the position of the *MN* using the range value between each *AN* and *MN* (this value includes errors that are generated with a Gaussian distribution). The result shows a position error of 2 m in the polar coordinate system if an error occurs within approximately 3 m, with a range error of 2 m occurring with position error of less than 1 m. With the proposed estimation algorithm described previously, this method can accurately determine the position of a *MN* within a mean error value of 1 m.

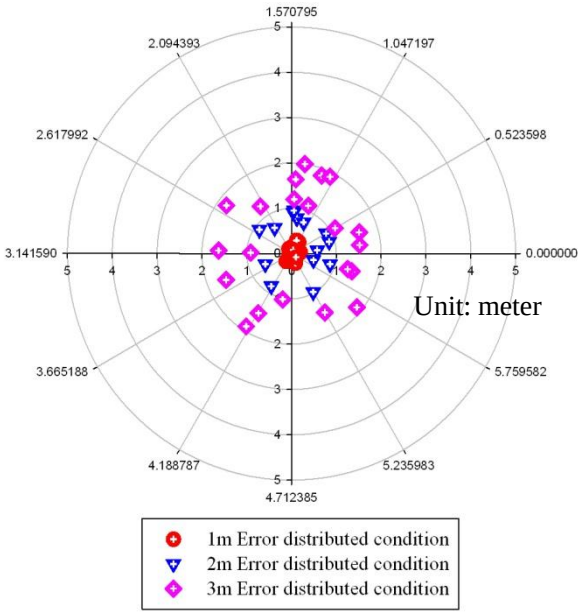

Fig. 9. Verifying the efficacy of the proposed algorithm under various distributed error conditions

5.2 Experimental evaluation

The *BSN*, *ANs* and *MNs* were deployed in order to evaluate the performance of our proposed location estimation method. IEEE 802.15.4a CSS ranging hardware equipped with an IEEE 802.15.4a CSS-compatible NanoLOC TRX transceiver [15] was installed in the experimental environments depicted in **Fig. 10**. The experimental environment was a distributed environment in which 8 *ANs* were located in a fixed position in a 100 × 35 m^2 rectangular office, depicted in **Fig. 10**. Furthermore, to identify the propagation condition of the experimental environment, we used the following simple signal propagation model:

$$P_{r_0} - P_{r_i} = 10\varepsilon \log(\frac{d_i}{d_0}) + v_i \tag{11}$$

Detailed characteristics of the path loss model are further given in [16]. In order to estimate the parameters of the path loss exponent, several training points were set in a wireless sensor network system. The value of ε as determined via the experiment was 5.21 in the office environment.

Fig. 10. CSS ranging hardware and installed AN

Fig. 11. Experimental environments: indoor office

We conducted experiments to determine the effect on the location accuracy of comparable methods for LOS/NLOS in multiple *MN* environments; the results of these experiments are graphically depicted. In addition, a test of every condition was conducted 200 to 250 times. It can be seen that our proposed method outperformed the conventional method, (the MLE technique that is based on the position grid method) under both LOS and NLOS conditions. In particular, in the NLOS environment, our proposed method proved highly superior to the conventional method as the localization error of the conventional method increased dramatically. That is because our proposed method utilizes not only the original ranging value source for localizing *MN*s by using linear regression analysis based on chirp spread spectrum but also the algorithm it uses has low complexity and high accuracy.

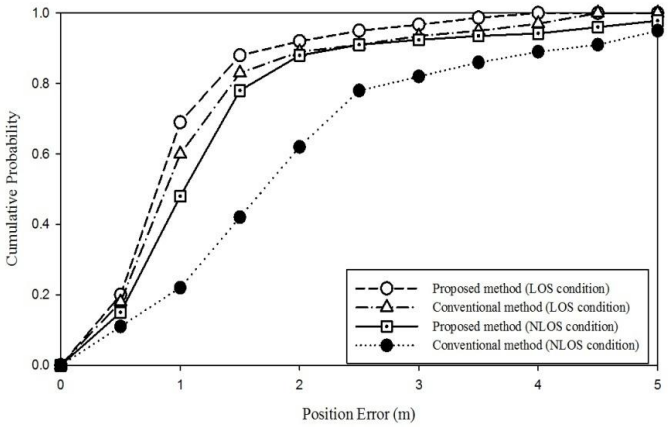

Fig. 12. Cumulative probability of position error

To investigate the scalability of our proposed localization algorithm, we performed experiments in which we varied the size of the test bed. The deployment areas had dimensions 30 m × 30 m, 30 m × 60 m, and 30 m × 90 m. **Fig. 13** shows the average computation time taken by the algorithm to update an *MN*'s position with respect to the number of *MN*s. As shown in **Fig. 13**, both of our proposed algorithm and the conventional algorithm proved sensitive to the number of *MN*s. The conventional algorithm is essentially a maximum likelihood technique that is based on statistical analysis, and its performance depends largely on the number of *MN*s. **Fig. 13 (c)** shows that the computation time taken by the conventional algorithm to update each *MN*'s position increased exponentially as the number of *MN*s increased. The experimental results also show that our proposed system updated position information within 60 ms, which indeed facilitate real-time tracking of mobile users with the MSP430-based sensor node. Furthermore, in the case of even 30 *MN*s, our proposed algorithm performed well; that is, it gave a reasonable performance in terms of computation time to update each *MN*'s position.

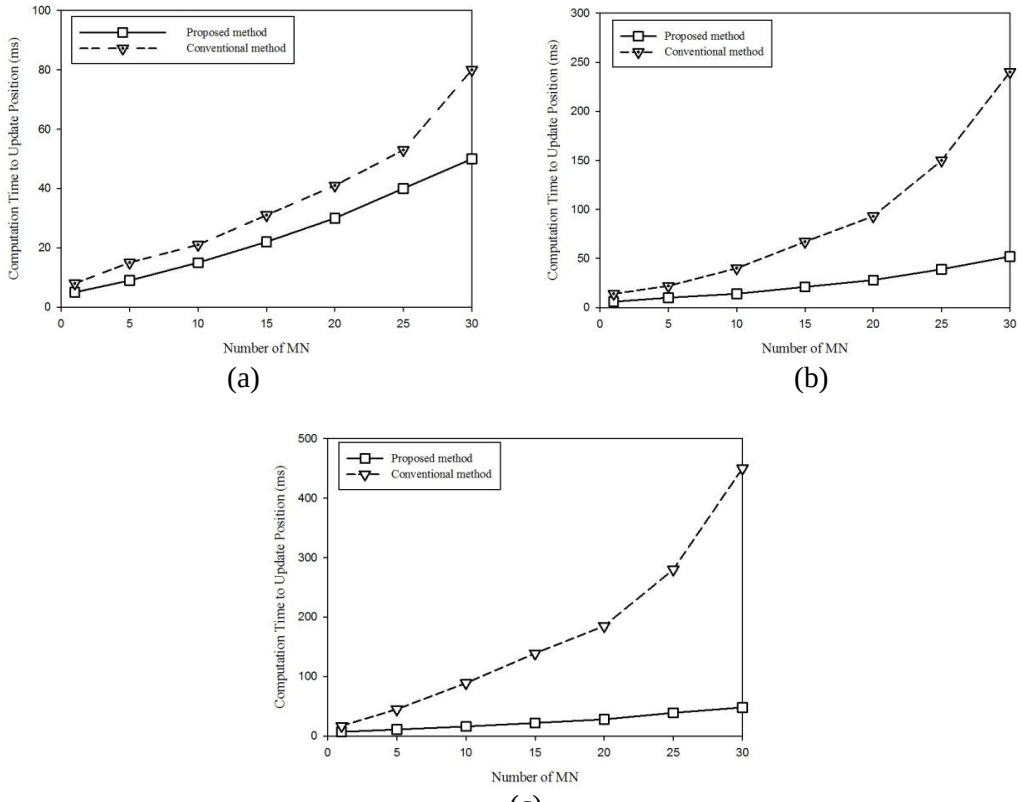

Fig. 13. Computation time to update each MN's position: (a) Small space-30 m × 30 m; (b) Medium space-30 m × 60 m (c); Large Space-30 m × 90 m

We then conducted an experiment in an actual environment. As shown in **Fig. 14**, the *MN* was assumed to be moving in the direction depicted by the line at the mean speed at which a human can move in each experimental environment. The figure compares the true trace with the locations estimated by applying the proposed method, as depicted by the dots. The results indicate that our proposed algorithm can achieve reasonably accurate tracking in NLOS propagation environments that are noisy.

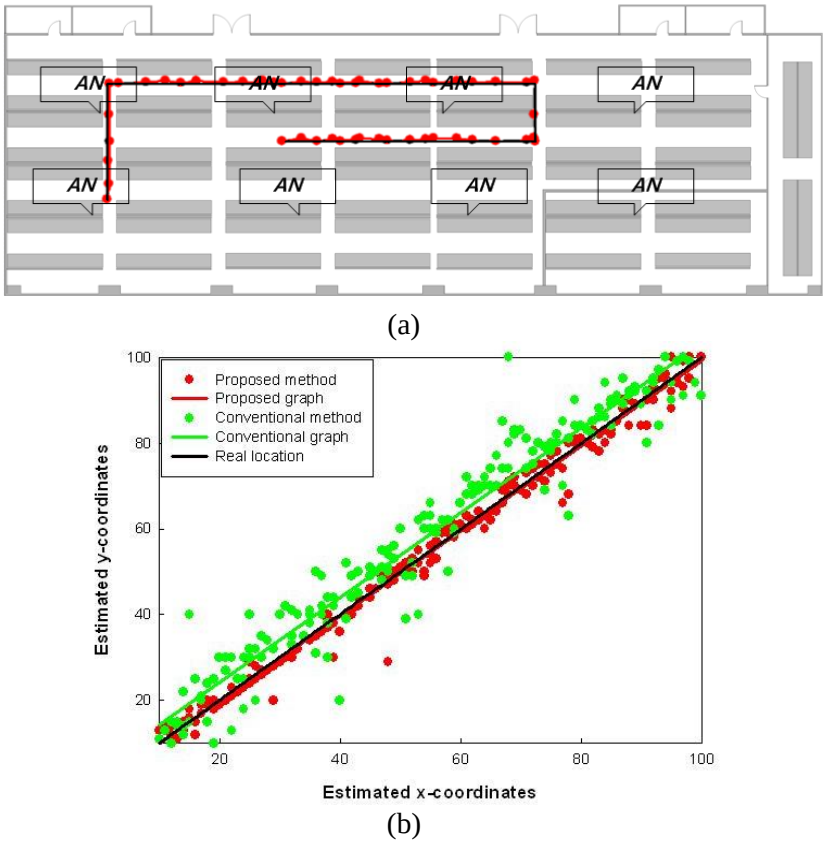

Fig. 14. Visualized tracking application in: (a) office and (b) distributed dotted plot

Fig. 15 shows the results obtained from experiments we conducted to determine the effect of the location accuracy in multiple *MN*s in fixed size office environments (in this case 100 m × 35 m). In this case also, each test was conducted a minimum of 200 times to a maximum of 250 times. As shown in **Fig. 15**, the result shows little difference between the proposed method and the conventional method. With only one *MN* operating in the experimental environment, as depicted in **Fig. 15 (a)** the positioning error remained within 1.3 m. The results of this experiment are in accord with the earlier simulation results, as depicted in **Fig. 9.**

We then conducted experiments with the more *MN*s in the same environmental condition. With 15 and 30 *MN*s, as depicted in **Fig. 15 (b)** and **(c)**, however, a significant difference was observed in the case of the conventional system: as the number of *MN*s increased, the device required additional ranging measurements, which could amplify the complexity of the network and create delays, whereas our proposed method had very little latency. Moreover, the conventional system required quite a significant processing time to overcome its deficiency, in this case the non-ideal measuring distance value, with high computational complexity based on its statistical method. In addition, the proposed method showed positional error within 1.8 m with 30 *MN*s. In summary, the experiment results, indicate that our proposed method for measuring range based on simple linear regression analysis and an algorithm with a self-calibration feature can achieve real-time tracking with high accuracy and low computational complexity.

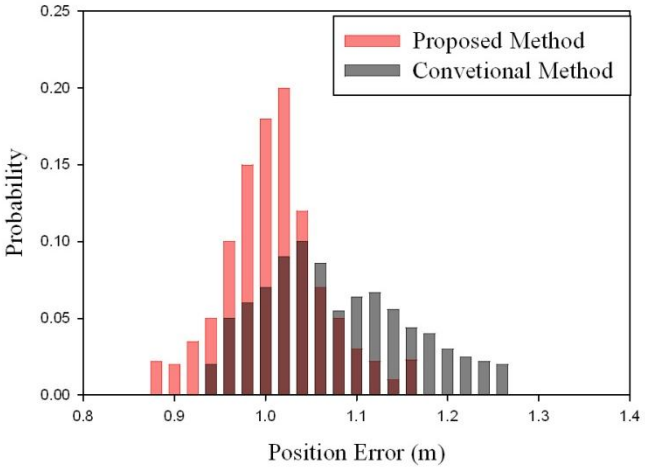

(a)

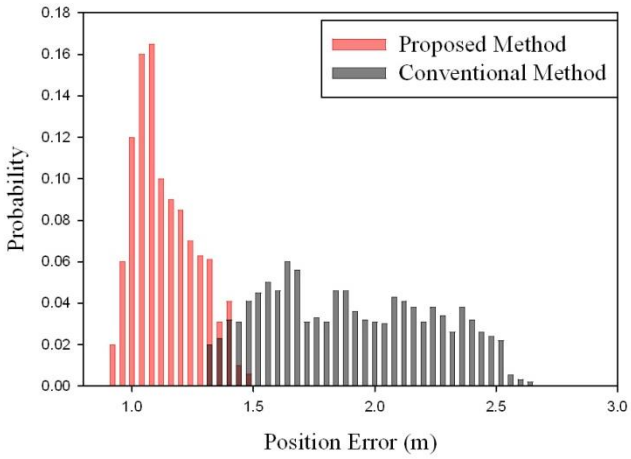

(b)

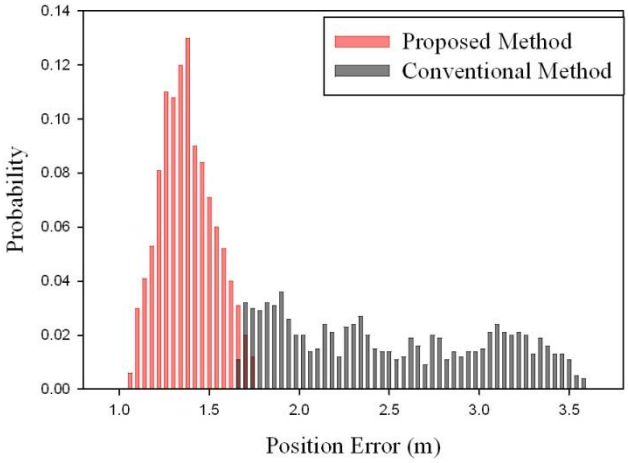

(c)

Fig. 15. Positioning error at the mobile node operation condition, with (a) 1 MN, (b) 15 MNs, and (c) 30 MNs

6. Conclusion

In this paper, we proposed an advanced localization system, that can operate multiple mobile nodes while guaranteeing a high level of positional accuracy even without *a priori* information about the location of the mobile devices. We applied a real-time simple linear regression model as the source for the localization of accurate range measurements. The proposed technique has low complexity as a result of its use of a simple linear regression method that utilizes the Big-$O(n^2)$ value for only 30 data points, within a 2 m range error. The proposed location estimation algorithm has a self-calibration feature to achieve enhanced accuracy and operation with multiple mobile nodes. To validate the feasibility of our method, we implemented the system in CSS ranging hardware comparable to IEEE 802.15.4a in an actual office environment. The results obtained indicate a mean error of approximately 1 m when multiple mobile nodes are operated concurrently. In conclusion, we have confirmed that our proposed localization system achieves high accuracy and low complexity during the operation of multiple mobile nodes with high positional accuracy in real environments.

References

[1] Hoshino, S., Ota, J., Shinozaki, A, and Hashimoto, H, "Hybrid Design Methodology and Cost-Effectiveness Evaluation of AGV Transportation Systems," *IEEE Transactions on Automation Science and Engineering*, vol. 4, pp. 360-372, July, 2007. Article (CrossRef Link).

[2] Xiaojing Huang, and Guo, Y.J., "Frequency-Domain AoA Estimation and Beamforming with Wideband Hybrid Arrays," *IEEE Transactions on Wireless Communications*, vol. 10, no. 8, pp. 2543-2553, August, 2011. Article (CrossRefLink).

[3] Stoica, L, Rabbachin, A., and Oppermann, I., "A low-complexity noncoherent IR-UWB transceiver architecture with TOA estimation," *IEEE Transactions on Microwave Theory and Techniques*, vol. 54, no. 4, pp. 1637-1646, June, 2006. Article (CrossRefLink).

[4] Chuan-Chin Pu and Wan-Young Chung, "Mitigation of Multipath Fading Effects to Improve Indoor RSSI Performance," *IEEE Sensors Journal*, vol. 8, no. 11, pp. 1884-1886, November, 2008. Article (CrossRefLink).

[5] Yu, K. and Guo, Y.J., "Statistical NLOS Identification Based on AOA, TOA, and Signal Strength," *IEEE Transactions on Vehicular Technology*, vol. 58, no. 1, pp. 274-286, January, 2009. Article (CrossRefLink).

[6] Peter J.Voltz and David Hemandez, "Maximum likelihood time of arrival estimation for real-time physical location tracking of 802.11 a/g mobile stations in indoor environments," *Position Location and Navigation Symposium*, pp.585-591, April 26-29, 2004. Article (CrossRefLink).

[7] Xinrong Li and Kaveh Pahlavan, "Super-resolution TOA estimation with diversity for indoor geolocation," *IEEE Transactions on Wireless Communications*, vol. 3, no. 1, pp. 224-234, January, 2004. Article (CrossRefLink).

[8] Fontana, R.J., Richley, E., and Barney, J. "Commercialization of an ultra wideband precision asset location system," in *Proc. of IEEE conference on Ultra wideband Systems and Technologies*, pp. 369-373, November, 2003. Article (CrossRefLink).

[9] Hernandez, A., Badorrey, R., Choliz, J., Alastruey, I., and Valdovinos, A., "Accurate indoor wireless location with IR UWB systems a performance evaluation of joint receiver structures and TOA based mechanism," *IEEE Transactions on Consumer Electronics*, vol. 54, no. 2, pp. 381-389, May, 2008. Article (CrossRefLink).

[10] Hyeonwoo Cho and Sang Woo Kim, "Mobile Robot Localization Using Biased Chirp-Spread Spectrum Ranging," *IEEE Transactions on Industrial Electronics*, vol. 57, no. 8, pp. 2826-2835, August, 2010. Article (CrossRefLink).

[11] Youngbae Kon, Yonggoo Kwon, Gwitae Park, "Robust Localization over Obstructed Interferences for Inbuilding Wireless Applications," *IEEE Transactions on Consumer Electronics*, vol. 55, pp. 105-111, April, 2009. Article (CrossRefLink).
[12] IEEE P802.15.4a/D4 (Amendment of IEEE Std 802.15.4), "Part 15.4: Wireless Medium Access Control (MAC) and Physical Layer (PHY) Specifications for Low-Rate Wireless Personal Area Networks (LRWPANs)," August, 2007. Article (CrossRefLink).
[13] K. Yedavalli, B. Krishnamachari, S. Ravula, and B. Srinivasan,"Ecolocation: A Sequence Based Technique for RF Localization in Wireless Sensor Networks," in *Proc. of 4th Int. Conf. on Information Processing in Sensor Networks*, pp. 285-292, April 25-27, 2005. Article (CrossRefLink).
[14] K. Yedavalli and B. Krishnamachari. "Sequence-Based Localization in Wireless Sensor Networks," *IEEE Transactions on Mobile Computing*, vol. 7, no. 1, pp. 81-94, January, 2008. Article (CrossRefLink).
[15] Nanotron Technologies GmbH, nanoLOC TRX Transceiver (NA5TR1) Datasheet, NA-06-0230-0388-2.00, Apr. 2008. Article (CrossRefLink).
[16] T.S. Rappaport, Wireless communications: Principles and Practice, 2nd Edition, Prentice Hall, 2002. Article (CrossRefLink).

Seong-Joong Kim was born in chung-ju, Korea, on November 30, 1988. He is now BS student in Computer Science and Engineering from Soongsil University, South Korea. Since 2008, he has been a member of the Convergent SoC Research Center, Korea Electronics Technology Institute (KETI) in South Korea. Also, in 2009, he joined the Samsung Electronics Software Membership as a student regular member, Seoul, South Korea.

Dong-Joo Park received the B.S. and M.S. degrees in the Computer Engineering Department from Seoul National University, February 1995 and February 1997, respectively, and the Ph.D. degree in School of CS&E from Seoul National University, August 2001. He is currently an associate professor in School of Computer Science and Engineering at Soongsil University. His research interests include flash memory-based DBMSs, multimedia databases, database systems, and embedded software.